

Relationships Between Calcalkalic and Alkalic Mineralization Styles at the Copper-Molybdenum Southeast Zone and Copper-Gold Deerhorn Porphyry Deposits, Woodjam Property, Central British Columbia (NTS 093A)

I. del Real, Mineral Deposit Research Unit, University of British Columbia, Vancouver, BC, idelreal@eos.ubc.ca

C.J.R. Hart, Mineral Deposit Research Unit, University of British Columbia, Vancouver, BC

F. Bouzari, Mineral Deposit Research Unit, University of British Columbia, Vancouver, BC

J.L. Blackwell, Gold Fields Canada Exploration, Vancouver, BC

A. Rainbow, Gold Fields Canada Exploration, Vancouver, BC

R. Sherlock, Gold Fields Canada Exploration, Vancouver, BC

del Real, I., Hart, C.J.R., Bouzari, F., Blackwell, J.L., Rainbow, A. and Sherlock, R. (2014): Relationships between calcalkalic and alkalic mineralization styles at the copper-molybdenum Southeast Zone and copper-gold Deerhorn porphyry deposit, Woodjam property, central British Columbia; *in* Geoscience BC Summary of Activities 2013, Geoscience BC, Report 2014-1, p. 63–82.

Introduction

Porphyry deposits of Late Triassic to Middle Jurassic age (216 to 183 Ma) occur in the Quesnel and Stikine terranes in British Columbia (McMillan et al., 1995). They are subdivided into calcalkalic and alkalic types on the basis of their hostrock chemistry and styles of alteration and mineralization (Lang et al., 1995; McMillan et al., 1995). Alkalic porphyry deposits such as Mount Milligan, Mount Polley and Lorraine, and calcalkalic porphyry deposits such as Brenda, Highland Valley and Gibraltar, among others, are examples of these two classes. These porphyry deposits commonly occur as clusters of several porphyry centres. The metal ratios, alteration assemblages and hostrock intrusive textures of each porphyry deposit can vary within each cluster (e.g., Casselman et al., 1995; Fraser et al., 1995). Such differences are commonly attributed to emplacement at different crustal depths of the now spatially related porphyry stocks (e.g., Panteleyev et al., 1996; Chamberlain et al., 2007). Recently, porphyry clusters such as Red Chris (Norris, 2011) and Woodjam (Figure 1) displaying both alkalic and calcalkalic features have been recognized. However, the genetic and spatial links between the various deposits in each camp, especially with contrasting assemblages (i.e., calcalkalic and alkalic) are not well understood.

The Woodjam property hosts several discrete porphyry deposits, including the Megabuck (Cu-Au), Deerhorn (Cu-Au), Takom (Cu-Au), Southeast Zone (Cu-Mo) and Three Firs (Cu-Au; Figure 2). These deposits display various

styles and assemblages of alteration and mineralization. Whereas the Southeast Zone Cu-Mo deposit is hosted in quartz monzonite intrusive units and displays alteration and mineralization comparable to calcalkalic porphyry deposits, the nearby Deerhorn Cu-Au deposit is associated with narrow (<100 m) monzonite intrusive bodies and hosts mineralization similar to alkalic porphyry deposits. These differences have resulted in the separation of the Southeast Zone (SEZ) from the Megabuck and Deerhorn deposits as a different mineralization event (Logan et al., 2011). However, similar ages of the host intrusive rocks (197.48 ± 0.44 Ma for SEZ and 196.35 ± 0.19 Ma for Deerhorn; Rainbow et al., 2013) and characteristics of alteration and mineralization suggest that deposits within the Woodjam property may be genetically related.

Recent exploration at the Deerhorn Cu-Au deposit has shown two contrasting alteration assemblages of K-feldspar+magnetite, typical of alkalic systems, and illite (\pm tourmaline) and Mo mineralization typical of calcalkalic systems. The SEZ, located less than 4 km from the Deerhorn deposit, displays some features not typical of calcalkalic deposits, such as infrequent quartz veining. These observations suggest that temporal and paragenetic relationships between the two deposits may exist, thus providing a unique opportunity to study the relationship between alkalic and calcalkalic deposits in BC.

Thus, a research project was jointly initiated in 2012 by the Mineral Deposit Research Unit at the University of British Columbia, Gold Fields Canada Exploration and Geoscience BC. The focus of this project is to increase the understanding of the paragenesis and alteration of the variable calcalkalic and alkalic deposits and the magmatic evolution in the Woodjam property. Results of this investigation will have important implications for the understanding of the

Keywords: *alkalic porphyry, calcalkalic porphyry, Woodjam property*

This publication is also available, free of charge, as colour digital files in Adobe Acrobat® PDF format from the Geoscience BC website: <http://www.geosciencebc.com/s/DataReleases.asp>.

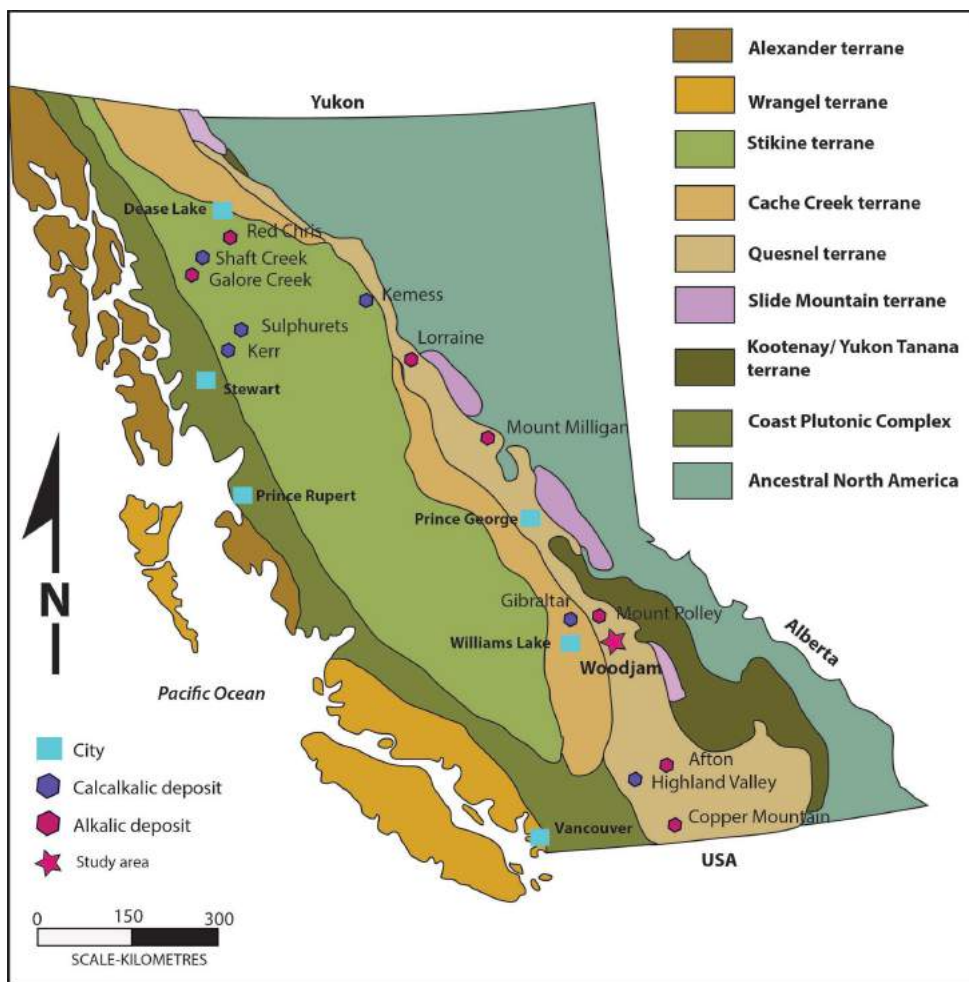


Figure 1. Major tectonic terranes and associated Mesozoic porphyry deposits of the Canadian Cordillera in British Columbia (from McMillan et al., 1995).

formation of porphyry clusters and the exploration of new targets in known mineralized districts in BC and similar regions worldwide.

Fieldwork focused on the SEZ and Deerhorn deposits and was carried out in summer 2012 and June 2013. A total of seven drillholes for the SEZ and ten for the Deerhorn deposit were graphically relogged (Figures 2, 3) and sampled. Hostrock texture, alteration assemblages and intensity, vein types and crosscutting relationships, sulphide ratios and shortwave infrared spectroscopy (SWIR) sampling were recorded and form the basis for ongoing detailed petrographic and chemical analyses. Paragenesis and alteration relationships were previously discussed on the basis of 2012 field observations (del Real et al., 2013). In this paper, results of the 2013 fieldwork, detailed geology and alteration cross-sections, petrography of the hostrocks and alteration assemblages, SWIR analysis and preliminary geochemical analyses are presented.

The Woodjam property is located in the Cariboo Mining Division, central British Columbia, approximately 50 km east-northeast of Williams Lake (Figure 1). The property is owned by Gold Fields Horsefly Exploration (51%) and Consolidated Woodjam Copper Corporation (49%). The Southeast Zone is the only deposit with a public pit-constrained resource estimated to be 146.5 Mt at 0.33% Cu (Sherlock et al., 2012).

Tectonic Setting

Much of BC comprises tectonic blocks that were accreted onto the western margin of ancient North America during the Mesozoic. Three of these accreted terranes, the Quesnel, Stikine and Cache Creek terranes, form most of the Intermontane Belt that occupies much of central BC (Figure 1; Monger and Price, 2002). The Stikine and Quesnel volcanic arc terranes have similar compositions and stratigraphy, and are interpreted to have originally been part of the same arc that was folded oroclinally, enclosing the Cache Creek terrane (Mihalynuk et al., 1994). Within the Quesnel

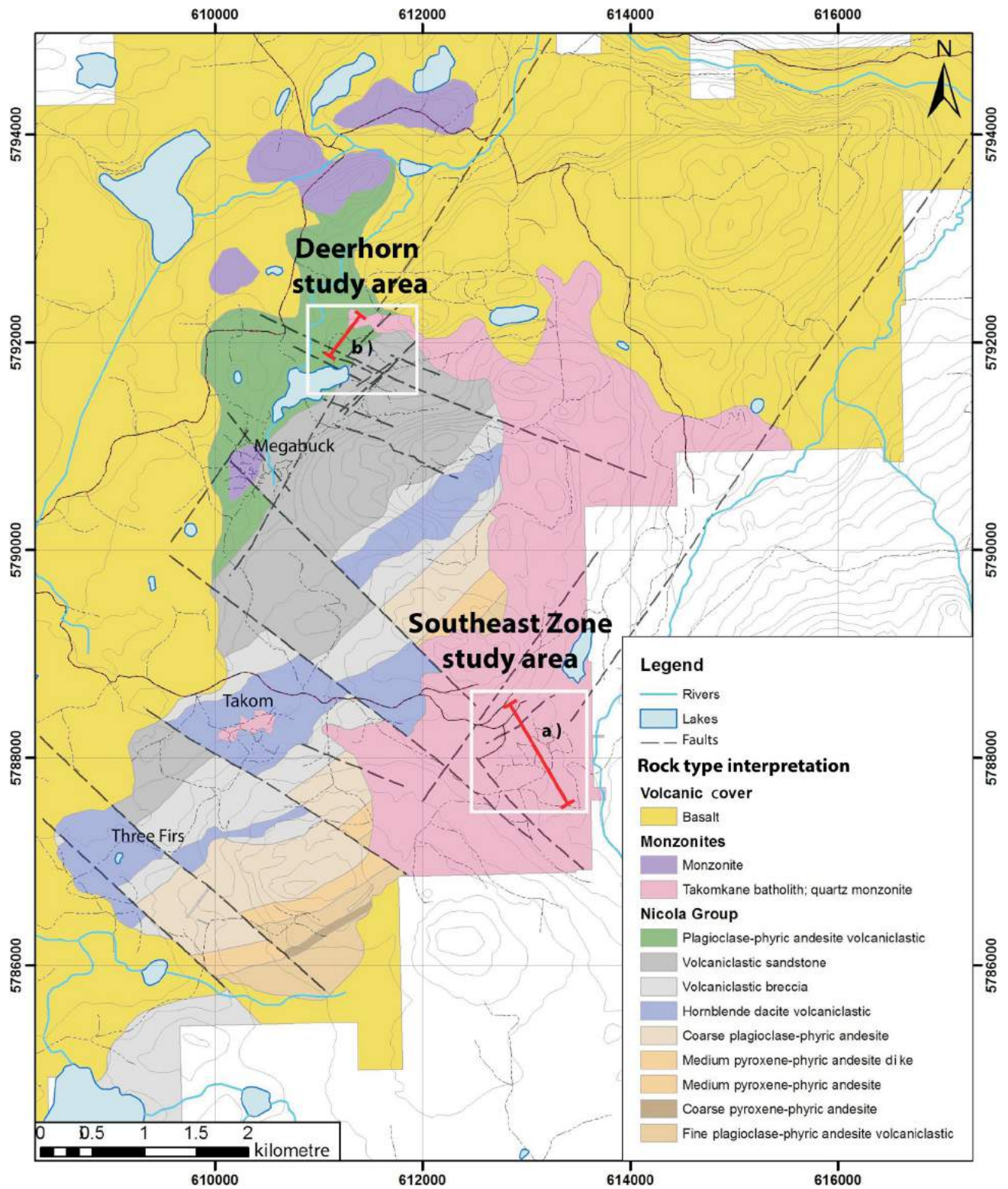


Figure 2. Geology of the Woodjam property. Cross-section lines of drillholes relogged in this study are shown (red line) for the **a)** Southeast Zone and **b)** Deerhorn deposits (from Gold Fields Canada Exploration, pers. comm., 2012).

and Stikine terranes, the emplacement of pre- to synaccretion of both alkalic and calcalkalic Cu±Mo±Au deposits, occurred between 216 and 187 Ma (McMillan et al., 1995). The Woodjam porphyry cluster is hosted in the Late Triassic to Early Jurassic arc in the central portion of the Quesnel terrane.

Regional Geology

The Quesnel terrane consists of upper Paleozoic and lower Mesozoic volcanic, sedimentary and plutonic rocks. The Paleozoic components are unconformably overlain by the Late Triassic and Early Jurassic island arc volcanic and sed-

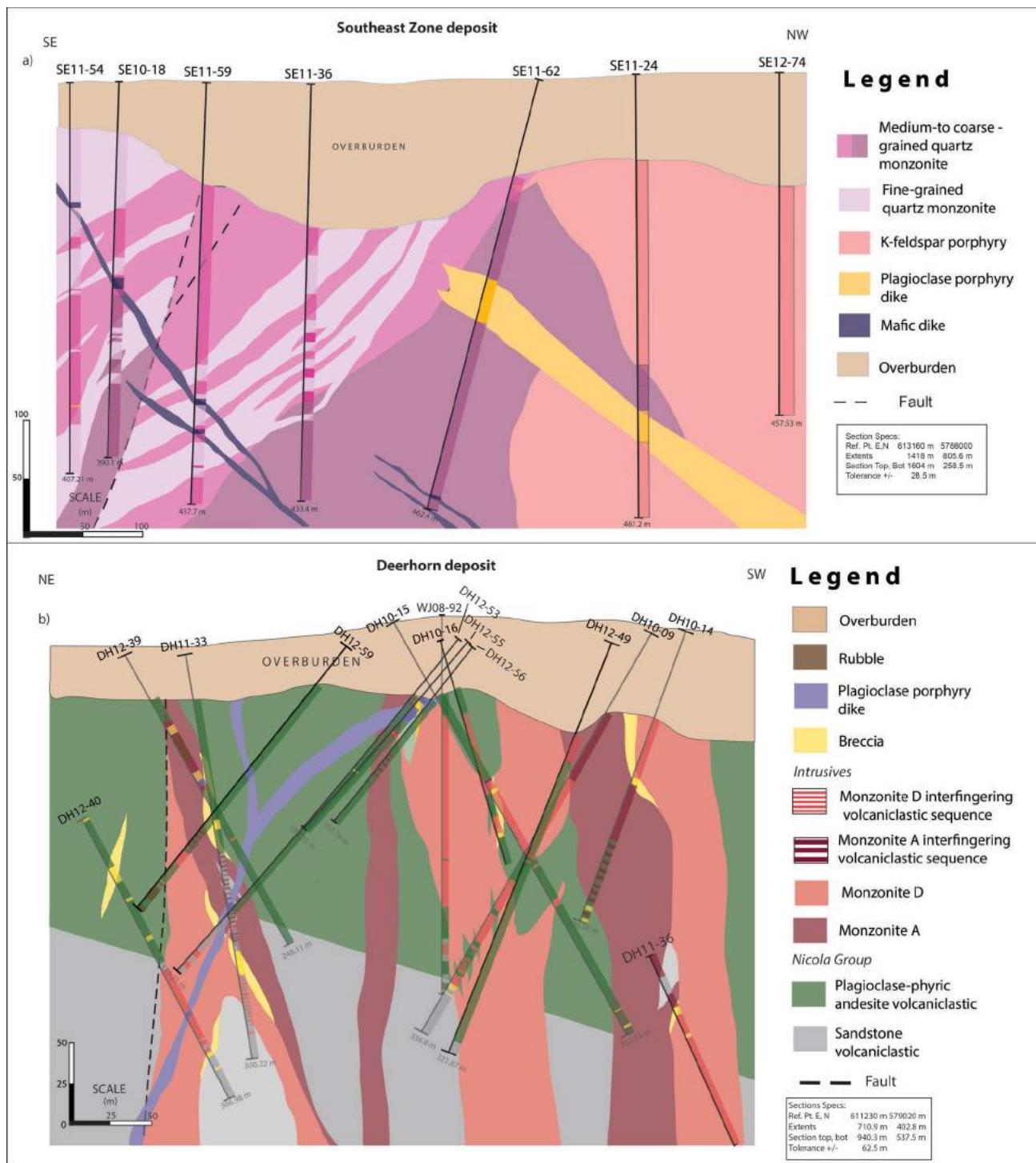


Figure 3. a) Southeast cross-section along the line 613160E, 5788000N, NAD 83, UTM Zone 10 (28.5 m thickness) across the Southeast Zone deposit; **b)** northeast cross-section along the line 611230E, 5792020N, NAD 83, UTM Zone 10 (62.5 m thickness) across the Deerhorn deposit.

imentary strata of the Nicola Group and its northern continuation, the Takla Group (McMillan, 1995). The Nicola Group is composed of submarine basaltic to andesitic augite±plagioclase±phyric lava and volcanoclastic and sedimentary units (Mortimer, 1987; Schiarizza et al., 2009; Vaca, 2012). This sequence extends throughout south-central BC.

These rocks were intruded by the Takomkane batholith, a largely calcalkalic intrusion of monzodiorite to granitoid, and locally quartz diorite, composition with a surface expression of approximately 40 by 50 km. The Woodjam Creek unit of the Takomkane batholith occurs on the Woodjam property and is composed of granodiorite, monzogranite and quartz monzonite (Schiarizza et al., 2009). The Nicola and Takomkane units are overlain by the Early Miocene to Early Pleistocene basalt of Chilcotin Group.

Geology of the Woodjam Property

The Woodjam property is hosted by a succession of Triassic–Jurassic Nicola volcanic and volcano-sedimentary rocks that are intruded by several Jurassic monzonite to syenite stocks. The Takomkane batholith occurs in the eastern and southern parts of the property (Figure 2) and mainly consists of light-grey to pinkish to white hornblende-biotite granodiorite, monzogranite, quartz monzonite and quartz monzodiorite (Schiarizza et al., 2009). Nicola Group rock units comprise a sequence of plagioclase±pyroxene±phyric andesitic rocks, monomictic and polymictic volcanic breccias, and volcanic mudstones and sandstones, all of which dip moderately to the northwest (Rainbow et al., 2013).

Locally, extensive olivine-phyric basalt flows of the Chilcotin Group are characterized by dark grey, aphanitic and vesicular basalt (Schiarizza et al., 2009). These flows range in thickness from less than 20 m to more than 100 m and overlie the Nicola stratigraphy.

Several zones of porphyry-type mineralization occur within and around porphyry stocks that intruded the strata of the Nicola Group. The SEZ deposit is hosted entirely in quartz monzonites of the Takomkane batholith, whereas the Deerhorn deposit is hosted by multiple monzonite intrusions and volcanic rocks of the Nicola Group (Rainbow et al., 2013; Sherlock et al., 2012).

Hostrock Geology

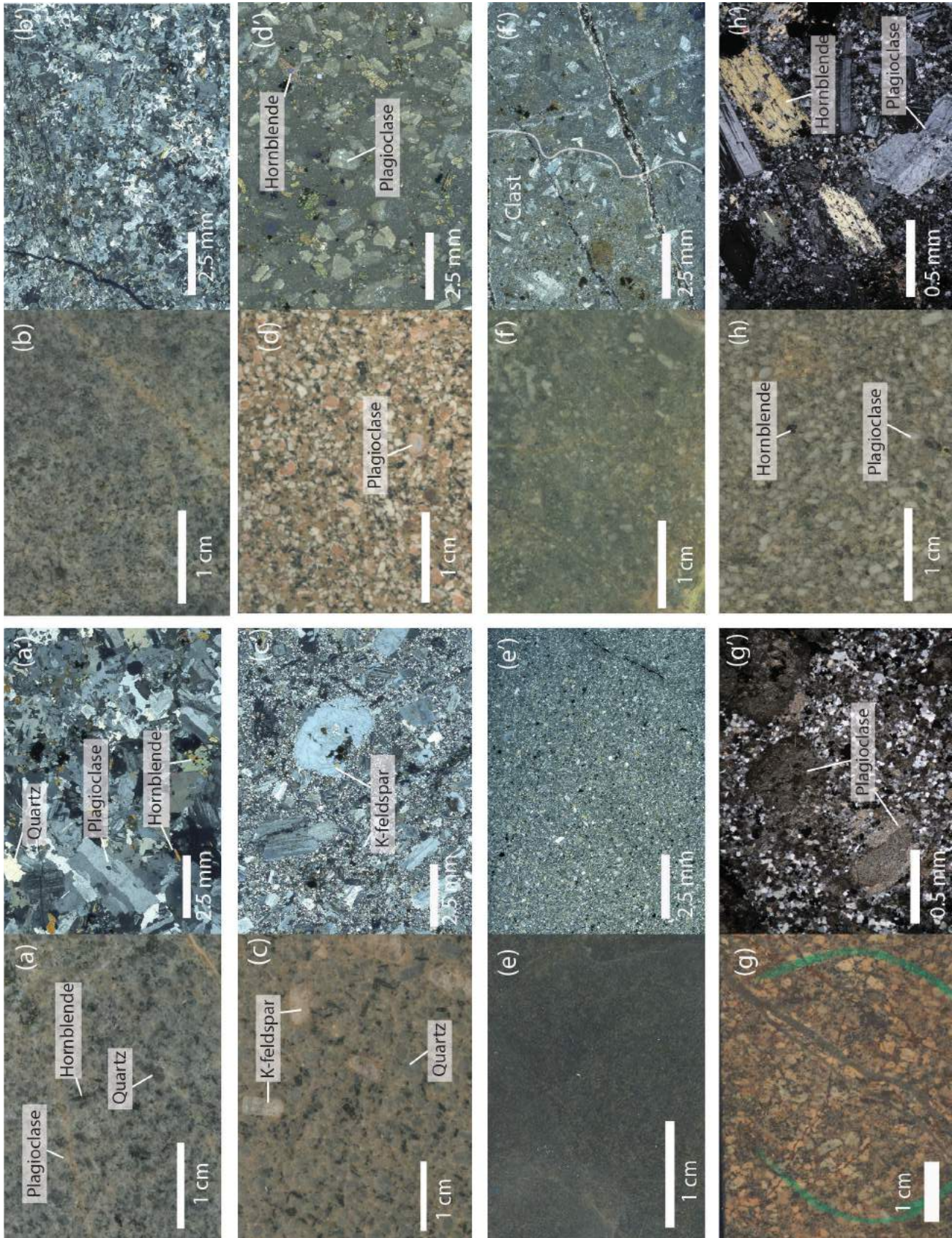
Southeast Zone Deposit

The Southeast Zone deposit is hosted by a series of texturally variable quartz monzonite intrusive units that strike ~220° and dip ~65–80° to the northwest (Rainbow, 2010). The quartz monzonites are divided texturally into fine-, medium- and coarse-grained units (Figures 3a, 4a, b; Rainbow, 2010). There is no textural or mineralogical difference be-

tween the coarse- and the medium-grained quartz monzonite, only the grain size varies. Fine-grained quartz monzonite cuts both medium- and coarse-grained intrusive rocks. Small aplite dikes cut all quartz monzonite units and the K-feldspar porphyry unit with sharp contacts. All quartz monzonite units are largely equigranular, white-grey to pink and comprise interlocking crystals of plagioclase (~40%), potassium feldspar (~15%) and quartz (~20%; Figure 4a, b). Mafic minerals are typically hornblende (~5%) and less abundant fine-grained biotite (~2%). Quartz monzonites are intruded by K-feldspar porphyry (FP) bodies characterized by a phaneritic medium- to coarse-grained groundmass, and large euhedral and elongated K-feldspar phenocrysts (~15%) that occur sporadically throughout the unit (Figure 4c). The FP forms a wide (>250 m), dike-like intrusion that strikes northeast (Rainbow, 2010; Sherlock et al., 2012). It cuts the quartz monzonite and has a chilled margin. All quartz monzonites were emplaced pre- to synmineralization and are affected by intense alteration, whereas the FP was probably emplaced during final stages of hydrothermal activity and is therefore typically weakly altered. All these units were intruded by postmineralization plagioclase porphyry dikes and late mafic dikes (Figures 3a, 4d; Rainbow, 2010; Sherlock et al., 2012).

Deerhorn Deposit

The Deerhorn deposit is hosted in both the volcano-sedimentary rocks of the Nicola Group and the monzonitic rocks that intrude the Nicola strata (Figure 3b; Scott, 2012; Rainbow et al., 2013). The host Nicola Group stratigraphy consists of laminated to thickly-bedded volcanoclastic sandstone (Figure 4e), overlain by a plagioclase-hornblende-phyric andesite that alternates between breccia and volcanic facies (Figures 3b, 4f; Rainbow et al., 2013). These units dip ~25° to the north in the deposit area and were intruded by at least two monzonite bodies. Monzonite A occurs as pencil-shaped intrusive bodies with irregular margins that intrude the volcano-sedimentary rocks of the Nicola Group (Figure 3b; Rainbow et al., 2013). Intense alteration obliterated much of the primary texture of monzonite A but remnants of plagioclase and biotite phenocrysts, altered to illite and chlorite, respectively, are locally recognizable (Figure 4g). Monzonite D is characterized by plagioclase (~35%), hornblende (~5%) and biotite (~5%) phenocrysts (Figure 4h) and occurs as dikes with sharp contacts that crosscut monzonite A and Nicola Group stratigraphy (Scott, 2012; Rainbow et al., 2013). The highest Cu and Au values occur in monzonite A and in the surrounding volcanic sandstone, where grades are locally ≤1.5 g/t Au and <0.75% Cu (Blackwell et al., 2012). Mineralization in monzonite D is mainly pyrite and subordinate chalcopyrite with Cu grades between 0.1 and 0.3% (Blackwell et al., 2012). Postmineralization mafic and andesitic dikes crosscut all the Deerhorn hostrocks and phases of mineralization (Rainbow et al., 2013).



Alteration

Hydrothermal alteration in both the Deerhorn and SEZ deposits affected all hostrocks except for postmineralization mafic and andesitic dikes. Several alteration assemblages are recognized in each deposit (Figures 5, 6, 7, 8). Short-wave infrared (SWIR) spectroscopy was used at both the SEZ and Deerhorn deposits to better characterize clay and white mica minerals and their distribution.

Southeast Zone

Potassium feldspar-biotite-magnetite is the earliest alteration assemblage in the SEZ deposit and typically occurs as pervasive alteration of K-feldspar replacing feldspar phenocrysts and biotite with magnetite replacing mafic minerals (Figures 5a, 6a, b). Potassium feldspar-biotite-magnetite alteration is very intense (i.e., nearly all original minerals and texture are destroyed) in the centre of the deposit, where secondary K-feldspar can make up to ~25% of the rock volume, biotite ~8% and magnetite ~7%. Weaker alteration at the margin of the deposit consists of secondary biotite (1%) and K-feldspar (5%), and magnetite is largely absent. Albite-(epidote) alteration is recognized at the northern extent of the deposit, where it is juxtaposed against K-feldspar-biotite-magnetite alteration by a large northeast-striking normal fault (Figures 3a, 8a). Albite alteration has a distinct bleached appearance and locally obliterates original rock textures (Figure 5b). In the deepest segment of the marginal area of the deposit, where albite alteration diminishes (~350 m depth), the K-feldspar-biotite-magnetite alteration assemblage appears and becomes more intense with depth, accompanied by higher grades of mineralization. The albite alteration is interpreted as having formed at the margin of the system, locally overprinting the K-feldspar-biotite-magnetite alteration. The albite alteration also occurs at the margin of the Takomkane batholith, near the contact with the Nicola Group strata (Figure 2). Both K-feldspar-biotite-magnetite and albite-(epidote) alterations are overprinted by epidote-chlorite-pyrite, illite and hematite alteration assemblages (Figure 5c).

Chlorite alteration appears throughout the SEZ, replacing secondary biotite and primary hornblende. Chlorite-epidote-pyrite veins are denser at the margins of the deposit. Epidote replaces plagioclase and occurs with hematite haloes at the margins of the deposit.

Illite occurs as three visually and paragenetically distinct types: dark green illite that replaces K-feldspar phenocrysts (Figure 5a); white illite that replaces plagioclase and commonly occurs with smectite; and apple-green illite (Figure 5c) that overprints albite and K-feldspar alterations, and occurs as flooding in the groundmass or as replacement of plagioclase. The white illite occurs mainly in fracture zones, together with hematite, and its distribution appears to be structurally controlled. Together with fracture-controlled white illite, hematite flooding largely occurs at shallow levels within the deposit (Figure 8a) as haloes to the epidote replacing plagioclase in the FP and as a pervasive alteration replacing secondary K-feldspar. Hematite overprints most of the previous alterations described above and also overprints(?) the plagioclase porphyry dike.

Deerhorn

Alteration assemblages at the Deerhorn deposit are strongly controlled by the distribution of the monzonites (Scott, 2012). Potassium feldspar-biotite-magnetite alteration (i.e., K-silicate) is very intense in monzonite A and in the volcanic rocks immediately surrounding these intrusions (Figures 5d, 8b). The intensity of the K-silicate alteration becomes progressively weaker in the surrounding volcanic rocks the farther it is from monzonite A. Monzonite D is only moderately affected by K-feldspar-biotite-magnetite alteration (Figure 6c, d), indicating that it postdated much of the main-stage alteration. The K-feldspar-biotite-magnetite alteration is overprinted by epidote-chlorite-pyrite, ankerite, calcite, illite and clay alteration assemblages. The epidote-chlorite-pyrite alteration occurs mainly in the surrounding volcanic rocks (Figures 5e, 6e, f, 8b) and, with less intensity, in monzonite D and in the plagioclase por-

Figure 4. Examples of hand samples, with corresponding thin-section photomicrographs (sample numbers represent drillhole numbers followed by depth) of hostrocks of the Southeast Zone (a, a', b, b', c, c', d, d') and Deerhorn (e, e', f, f', g, g', h, h') deposits showing: **a)** and **a')** medium-grained quartz monzonite with porphyritic texture; plagioclase phenocrysts are subhedral and up to 5 mm long; hornblende is subhedral and up to 1 mm long; quartz is anhedral and up to 3 mm long; and K-feldspar is anhedral and up to 3 mm in length or diameter (SE11-36; 285.55 m); **b)** and **b')** fine-grained quartz monzonite showing equigranular texture with subhedral plagioclase and hornblende phenocrysts, and anhedral K-feldspar and quartz, with grain size between 0.5 and 1 mm (SE11-36; 276.59 m); **c)** and **c')** K-feldspar porphyry, displaying porphyritic texture and characterized by abundant, large (up to 1 cm) K-feldspar, plagioclase (up to 0.7 cm) and quartz (up to 0.7 cm) phenocrysts; K-feldspar and plagioclase phenocrysts are subhedral, whereas quartz is anhedral (SE11-24; 260.2 m); **d)** and **d')** plagioclase porphyry dike, with plagioclase (up to 4 mm) and rare hornblende (up to 3 mm) phenocrysts in a very fine-grained groundmass (SE11-24; 285.55 m); **e)** and **e')** volcanoclastic sandstone with very fine-grained texture and reworked subhedral plagioclase crystals (DH12-40; 347.5 m); **f)** and **f')** plagioclase-hornblende-phyric andesite with local clast-breccia facies showing porphyritic texture with plagioclase phenocrysts (subhedral and up to 3 mm long); clast boundaries in the breccia facies are difficult to recognize (DH10-14; 105.7 m); **g)** and **g')** monzonite A with very strong alteration making it difficult to recognize the texture and the original mineralogy of the rock, and showing porphyritic texture with plagioclase phenocrysts up to 5 mm long mostly altered to illite; groundmass is altered to secondary K-feldspar (DH10-09; 79.5 m); **h)** and **h')** monzonite D showing porphyritic texture with plagioclase (subhedral and up to 5 mm long), hornblende (subhedral and up to 2 mm long) and biotite (subhedral and up to 2 mm long) phenocrysts; the groundmass is fine-grained plagioclase (DH12-39; 178.9 m).

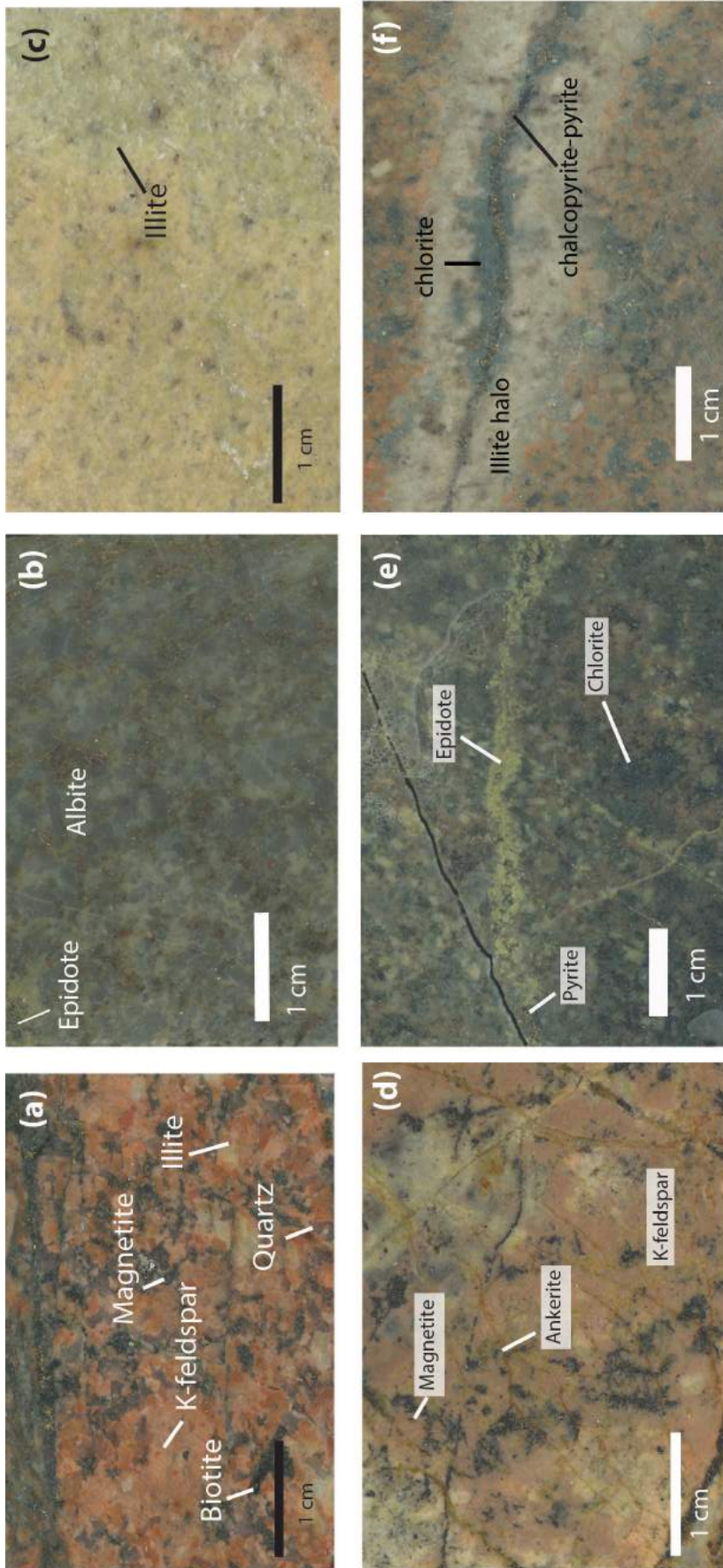


Figure 5. Selected drillcore samples showing alteration assemblages at the Southeast Zone (a, b, c) and Deerhorn (d, e, f) deposits: **a)** intense K-feldspar–biotite–magnetite alteration in coarse-grained monzonite locally overprinted by illite; **b)** very intense pervasive albite–(epidote) alteration texture, destructive in medium-grained monzonite; **c)** apple-green pervasive illite alteration overprinting albite and K-feldspar–biotite–magnetite alterations in fine-grained quartz monzonite; **d)** intense K-feldspar–biotite–magnetite alteration in the volcanic hostrock near the contact with monzonite A overprinted by illite and cut by late ankerite veins; **e)** epidote and quartz-pyrite veins in the volcanoclastic andesite hostrock; **f)** illite-vein envelope of chalcopyrite stringer in monzonite D cutting K-silicate alteration.

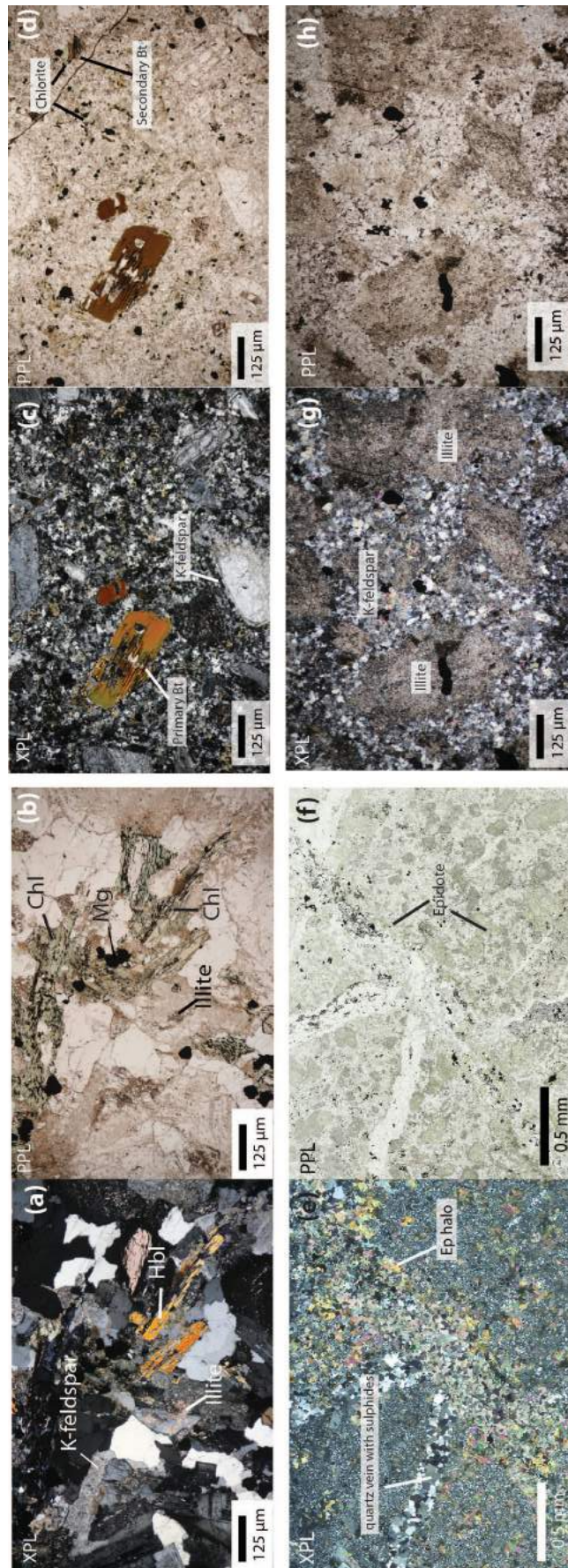


Figure 6. Photomicrographs showing alteration assemblages at the Southeast Zone (a, b) and Deerhorn (c, d, e, f, g, h) deposits: **a)** intense K-feldspar–biotite–magnetite alteration in coarse-grained monzonite; illite has partially replaced K-feldspar (XPL); **b)** intense K-feldspar–biotite–magnetite alteration in coarse-grained monzonite; biotite has replaced hornblende and, in turn, has been replaced by chlorite (PPL); **c)** and **d)** monzonite D moderately altered by K-feldspar–biotite–magnetite alteration, showing chlorite alteration replacing secondary biotite; **e)** and **f)** epidote-vein envelope of a late quartz vein that is cutting an early quartz vein with sulphides in the volcanic hostrock; **g)** and **h)** illite selectively replacing plagioclase and overprinting K-feldspar alteration in monzonite A. Abbreviations: bt, biotite; chl, chlorite; ep, epidote; hbl, hornblende; mg, magnetite; PPL, plain polarized light; XPL, crossed polarized light.

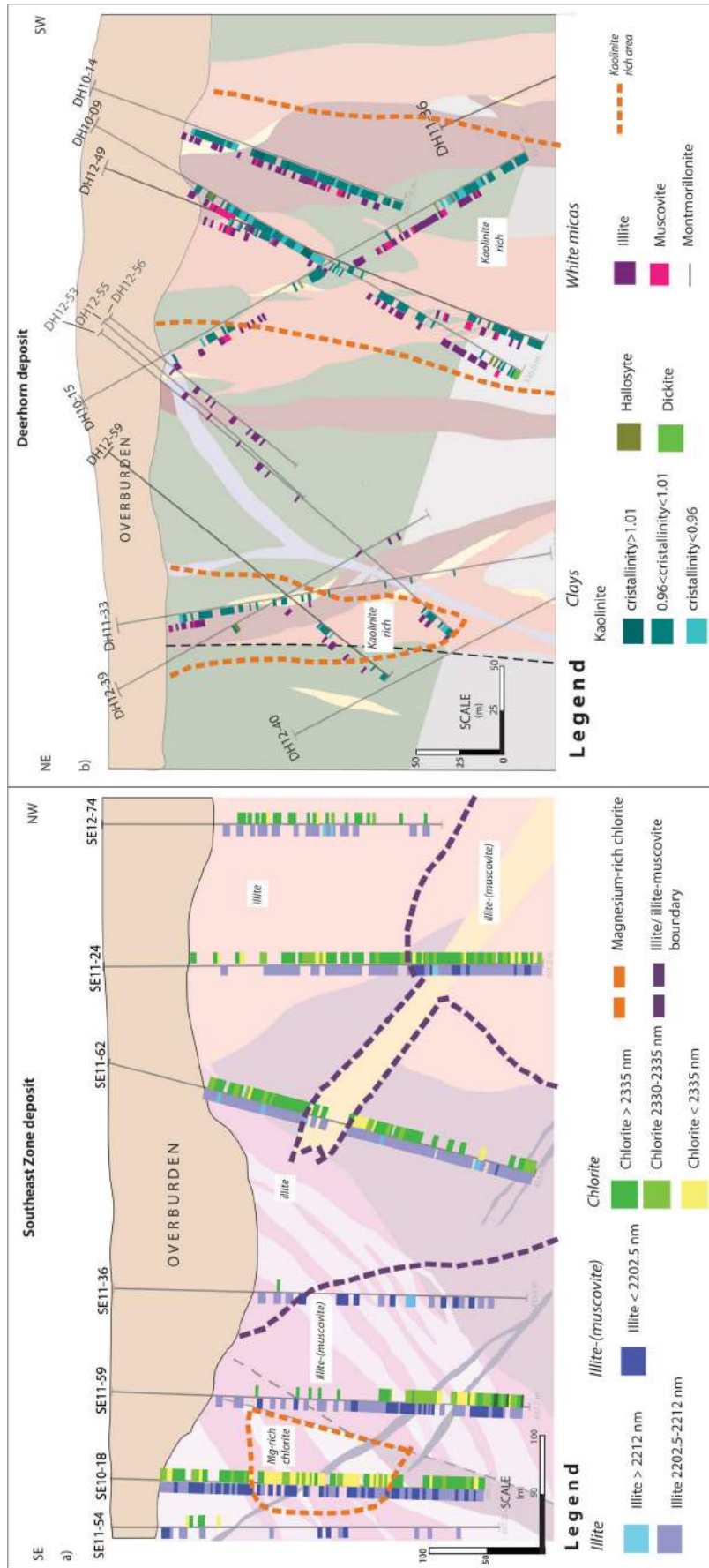


Figure 7. Results of the shortwave infrared spectroscopy (SWIR) analysis of drillhole samples from: a) the Southeast Zone deposit, showing illite and chlorite; b) the Deerhorn deposit, showing various domains of clay and white mica alteration.

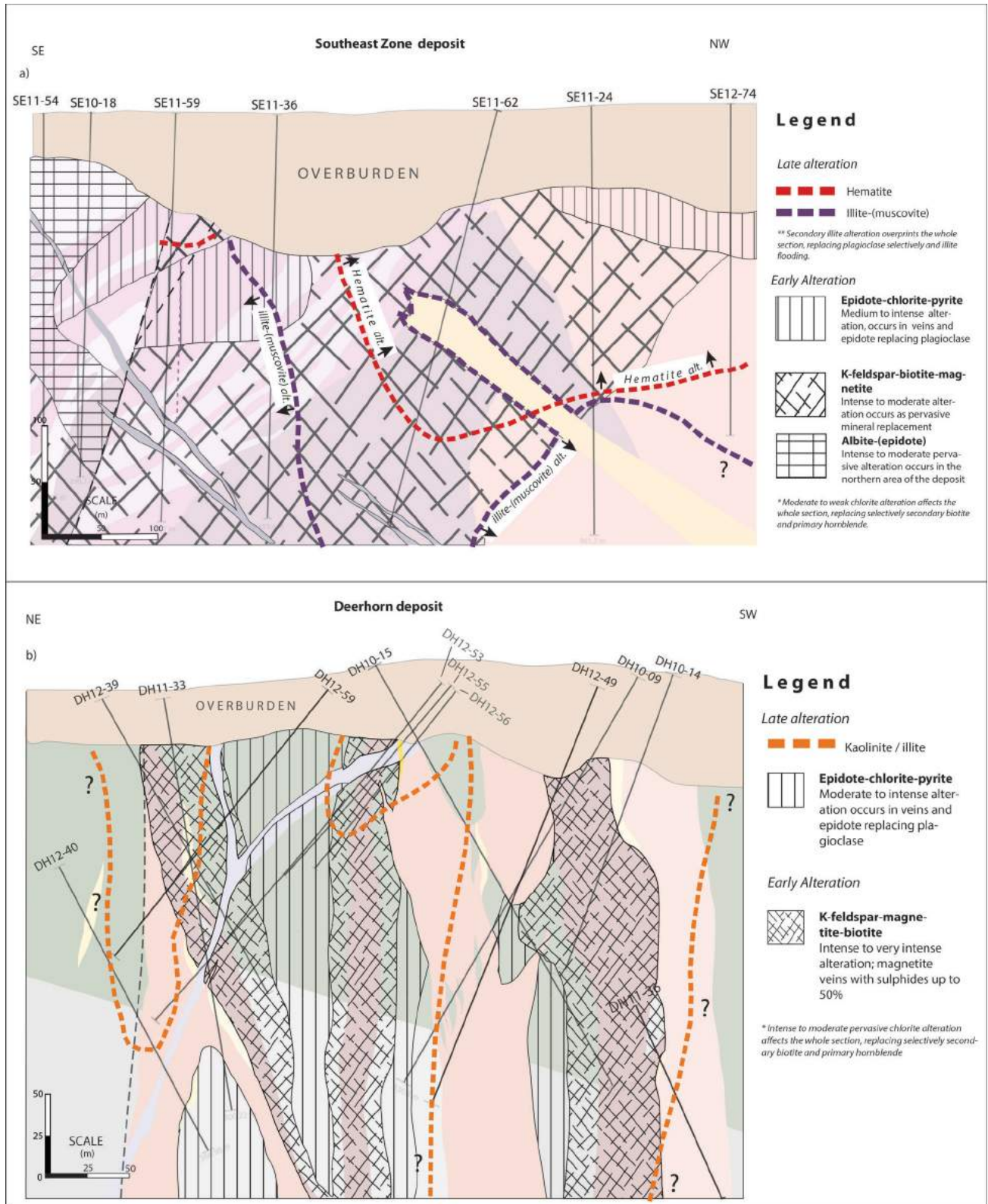


Figure 8. Cross-section of the a) Southeast Zone and b) Deerhorn deposits showing main alteration assemblages.

phyry dike. The alteration assemblage occurs as veins and disseminations (Figure 8b). Chlorite alteration occurs everywhere in the deposit, replacing secondary and primary biotite and primary hornblende.

Light green to white illite occurs as a replacement of plagioclase (Figure 6g, h) and as vein envelopes overprinting K-feldspar haloes (Figure 5f).

Ankerite and calcite veinlets occur throughout all rock types but commonly not together or in the same vein paragenesis. Ankerite occurs in the northeastern part of the area represented by the cross-section, whereas calcite occurs in the centre and southwestern parts. The observed spatial separation between the ankerite and calcite veinlets could be related to the different hostrocks. Ankerite appears related to the northeastern intrusion body of monzonite A, whereas calcite appears to be related to the other intrusive bodies of monzonite A.

Methods

Shortwave infrared (SWIR) spectroscopy is based upon reflectance and absorption patterns as light with wavelengths between 1300 and 2500 nm interacts with molecular bonds matching the specific wavelengths for molecules, such as OH, H₂O, AlOH, MgOH and FeOH (Thompson et al., 1999). Two instruments were used in this study: the TerraSpec[®] high-resolution spectrometer made by Analytical Spectral Devices Inc., which uses a 6 nm resolution and enhanced performance in SWIR 1 and 2 regions to characterize alteration assemblages, and the TerraSpec unit from the University of British Columbia (UBC), which is also used for characterizing alterations assemblages, but which is less portable.

Southeast Zone Deposit

Shortwave infrared spectra of the SEZ deposit were collected in the field using the portable TerraSpec instrument. Measurements were taken every 2 m along the drillcore, except for hole SE11-36 and the first half of holes SE11-59 and SE11-54, where measurements were collected every 7 m, mainly because samples had to be carried to Vancouver for analysis. Samples were measured at UBC also using a TerraSpec instrument. Results were interpreted using spectral features of the minerals, such as wavelength and depth. These analyses show illite and chlorite as the most common alteration(?) phases.

Chlorite spectra at the deposit margin registered a relatively higher 2250 nm absorption feature (corresponding to the FeOH feature) and is therefore more Mg-rich here (Figure 7a). Illite can be divided into two major groups on the basis of the AlOH absorption feature: the first group with a signature of <2201 nm and the second, with a signature of >2201 nm (Figure 7a). The first group corresponds to an

illite-(muscovite) assemblage with a K-rich affinity and occurs at the margins of the deposit surrounding the more intense K-feldspar–biotite–magnetite alteration. The second group corresponds to illite with a slightly phengitic affinity that overprints the entire deposit, but is more widespread in the central parts. These results correlate with petrographic observations: SWIR data suggest that illite with a phengitic affinity corresponds to the dark green illite that replaces plagioclase (Figure 5a) and the apple-green illite (Figure 5c) corresponds to the illite-(muscovite).

Deerhorn Deposit

At the Deerhorn deposit, SWIR data were collected in the field from cores samples measured in drillholes at 2 m intervals with the portable TerraSpec instrument. Analysis of this data identified chlorite, illite, montmorillonite and kaolinite. The SWIR technique was especially useful for identifying montmorillonite and kaolinite, which were difficult to visually identify during core logging. SWIR results for illite, based on the shifts of the AlOH absorption feature located at about 2200 nm, show the presence of K-rich affinity illite at the Deerhorn deposit, versus the illite at the SEZ. The SWIR analysis results also show a higher presence of muscovite in the Deerhorn deposit relative to that in the SEZ (Figure 7b). Core samples in the Deerhorn deposit are dominated by the presence of montmorillonite and kaolinite. Montmorillonite occurs in all the samples and kaolinite is more common in the northeastern part of the deposit (Figure 7b) along a major structure (Blackwell et al., 2012). Therefore, distribution of the kaolinite appears to be structurally controlled, overprinting illite and muscovite. This alteration seems to be part of a secondary alteration process involving meteoric fluids that used the structures as conduits. This observation stems mainly from the fact that the presence of kaolinite alteration was noted, along with dusty hematite replacing magnetite and secondary chalcocite replacing chalcopyrite that likely formed during supergene alteration.

Vein Types and Paragenesis

Southeast Zone Deposit

The earliest veins in the SEZ deposit are rare magnetite stringers and quartz-chalcopyrite-magnetite veins. These veins occur locally in the core of the porphyry (Figure 5a; Figure 9a). In the deep central and marginal areas of the SEZ, fewer (two to eight veins per metre) quartz-chalcopyrite-pyrite±molybdenite±anhydrite (±bornite) veins, locally with K-feldspar haloes, and chalcopyrite-pyrite stringer veins occur (Figure 9b). Pyrite-epidote-chlorite veins (Figure 9c), with epidote±hematite±illite haloes, are the youngest veins that host pyrite with minor chalcopyrite and cut all earlier veins. Quartz-chalcopyrite-pyrite±molybdenite±anhydrite veins, with and without K-feldspar haloes, dominate areas with stronger K-feldspar–biotite–

magnetite alteration but progressively become less abundant toward the margins of the deposit. Pyrite-epidote-chlorite veins occur most commonly at the margins of the deposit, and are associated with the intense epidote±chlorite±pyrite alteration assemblage of the hostrocks. They are rare to absent in the central parts of deposit. Pre- to syn-

mineralization veins such as magnetite, quartz±magnetite±chalcopyrite, and quartz±anhydrite veins with sulphides, and with and without K-feldspar haloes, commonly occur in all quartz monzonite units but are less abundant in the K-feldspar porphyry unit. This unit is largely cut by late pyrite±epidote±chlorite veins, indicating that the K-feldspar

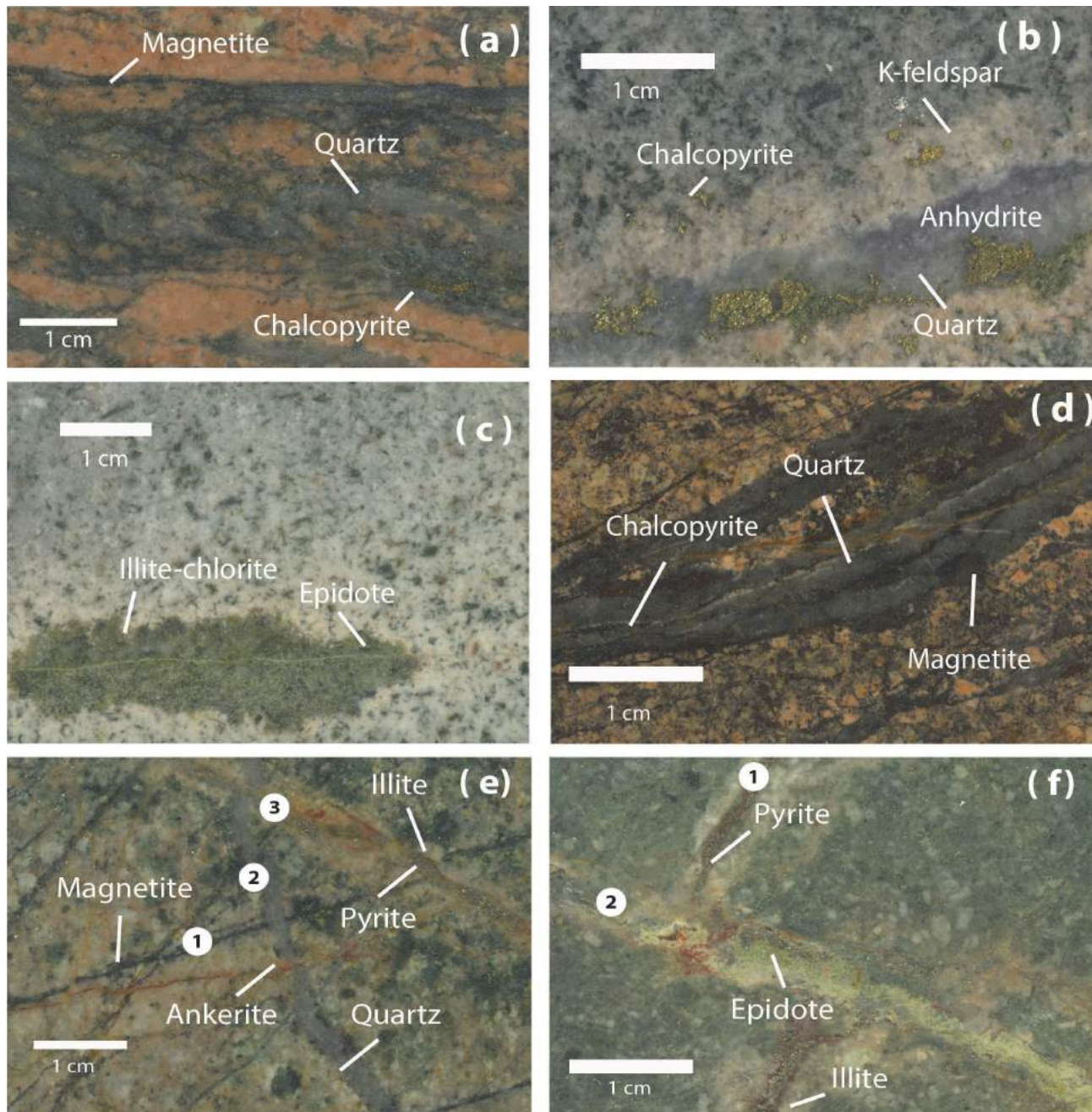


Figure 9. Schematic representation of vein assemblages in the Southeast Zone (a, b, c) and Deerhorn (d, e, f) deposits (sample numbers represent drillhole numbers followed by depth): **a)** quartz-magnetite-chalcopyrite veins with very intense K-feldspar–biotite–magnetite alteration in the coarse-grained quartz monzonite (SE11-62; 185.08 m); **b)** quartz-chalcopyrite-molybdenite-pyrite-anhydrite vein with K-feldspar halo in the medium-grained quartz monzonite with disseminated chalcopyrite occurring near mafic minerals (SE11-59; 278.49 m); **c)** epidote-chlorite vein with illite halo (SE11-54; 54 m); **d)** magnetite stockwork and Au-bearing quartz-magnetite-chalcopyrite banded veins in monzonite A (DH10-09; 79.5 m); **e)** magnetite stockwork cut by a quartz-magnetite vein (1), an illite-pyrite-hematite vein (2) and an ankerite vein (3) in monzonite A (DH10-09; 263.2 m); **f)** pyrite-quartz-hematite vein with illite halo (1) cut by a pyrite-chlorite-epidote vein (2) in hostrock (DH12-39; 178.19 m).

porphyry unit is younger than the quartz monzonites and postdates at least part of the main phase of mineralization. All these veins are cut by late carbonate veins.

Deerhorn Deposit

In the Deerhorn deposit, early magnetite stockwork and banded, Au-bearing quartz-magnetite-chalcopyrite±hematite veins with sulphides (Figure 9d) commonly occur in monzonite A and the adjacent volcanic hostrock. Monzonite D cuts monzonite A and the early Au-bearing quartz-magnetite veins with sulphides. Abundance and mineral proportion of early quartz-magnetite±hematite veins with sulphides vary from high-density and sulphide-rich in monzonite A and the surrounding volcanic rocks to a paucity of sulphides and lower abundance of veins distally. Similar relationships were observed for the early magnetite stockwork. Quartz veins with sulphides, and with and without K-feldspar haloes, occur throughout all units and cut the early quartz-magnetite veins with sulphides (Figure 9e). Locally, quartz veins with sulphides have an illite overprint of a K-feldspar halo, which is interpreted as a later event (Figure 9e). Pyrite-quartz±hematite±epidote veins with white illite haloes, and in less abundance tourmaline, occur throughout all rock units, cutting early veins and being cut in turn by pyrite-chlorite±epidote±calcite±ankerite veins (Figure 9f). Tourmaline was identified locally during this study (in hole DH10-09 at 150 m and DH12-49 at 295 m) occurring in monzonite D or volcanic hostrock near monzonite D. It occurs as a dark grey alteration (Figure 10a) or as black subhedral crystals surrounding a pyrite vein (Figure 10b). Late carbonate and hematite veins occur throughout all hostrocks, including late mafic dikes. These observations indicate that pre- to synmineralization veins such as the Au-bearing quartz-magnetite veins with sulphides occur mainly in monzonite A and in volcanic hostrock adjacent to it, whereas monzonite D is commonly cut by late veins.

A summary of the various vein types and timing relationships observed for each deposit is presented in Figure 11.

Mineralization

Copper, gold and molybdenum mineralization in the Woodjam property are controlled by the hostrock, alteration, density of veining and location (margins or central area) within the porphyry system. In the SEZ deposit, Cu occurs dominantly in chalcopyrite with subordinate bornite disseminated but more commonly in veins (Figure 9a, b). Molybdenite is observed mainly in veins. Sulphide minerals occur in quartz veins and chalcopyrite-pyrite stringer veins as fine-grained and anhedral grains, whereas sulphide disseminations in the hostrock are intimately related to mafic mineral sites. Areas of high Cu grades (~0.5%; Figure 12a) are characterized by dense stockworks of thin veins and abundant disseminated chalcopyrite in the hostrock. Copper grades decrease with depth (to <0.4% by ~300 m; Figure 12a) as chalcopyrite-pyrite stringer veins become less abundant to absent and Cu mineralization becomes more concentrated in quartz veins (up to 2 cm wide) with K-feldspar haloes. Gold mineralization (less than 1 ppm, rarely up to 4 ppm) may be associated with banded dark quartz-magnetite-chalcopyrite veins that occur in the core of the porphyry deposit.

Sulphide zoning at the SEZ consists of a chalcopyrite±bornite (±pyrite; hole SE11-62) assemblage in the core of the deposit, which changes upward and outward to chalcopyrite±molybdenite±pyrite (holes SE11-59 and SE11-36) and finally, a pyrite-dominated assemblage in the periphery of the deposit (holes SE10-18, SE11-24, SE12-74 and SE11-54). The pyrite:chalcopyrite (py:cpy) ratio defines zones with an approximately southwest orientation similar to the trend of the basalt and andesite porphyry dikes (Figure 12a). In the northwestern part of the deposit, where the FP intrudes, chalcopyrite is less abundant but still shows a

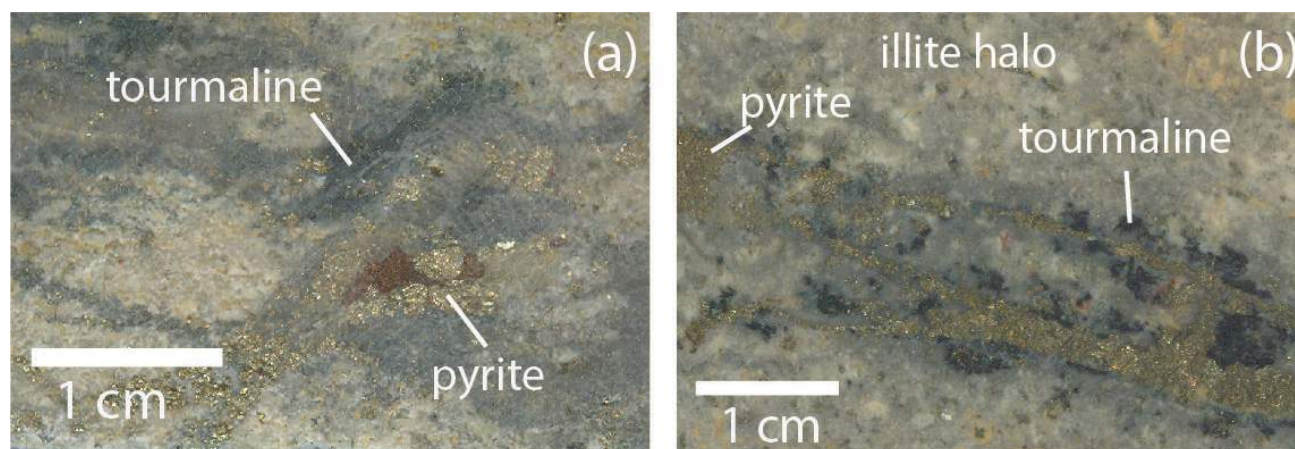


Figure 10. Pyrite-quartz±hematite±epidote±illite halo (±tourmaline halo) vein examples with tourmaline halo, showing **a)** dark grey anhydrous tourmaline surrounding a pyrite veinlet (DH10-09; 150 m) in monzonite D; **b)** black subhedral tourmaline surrounding a pyrite vein with an illite halo in volcanic hostrock (DH12-49; 295 m). Sample numbers represent drillhole numbers followed by depth.

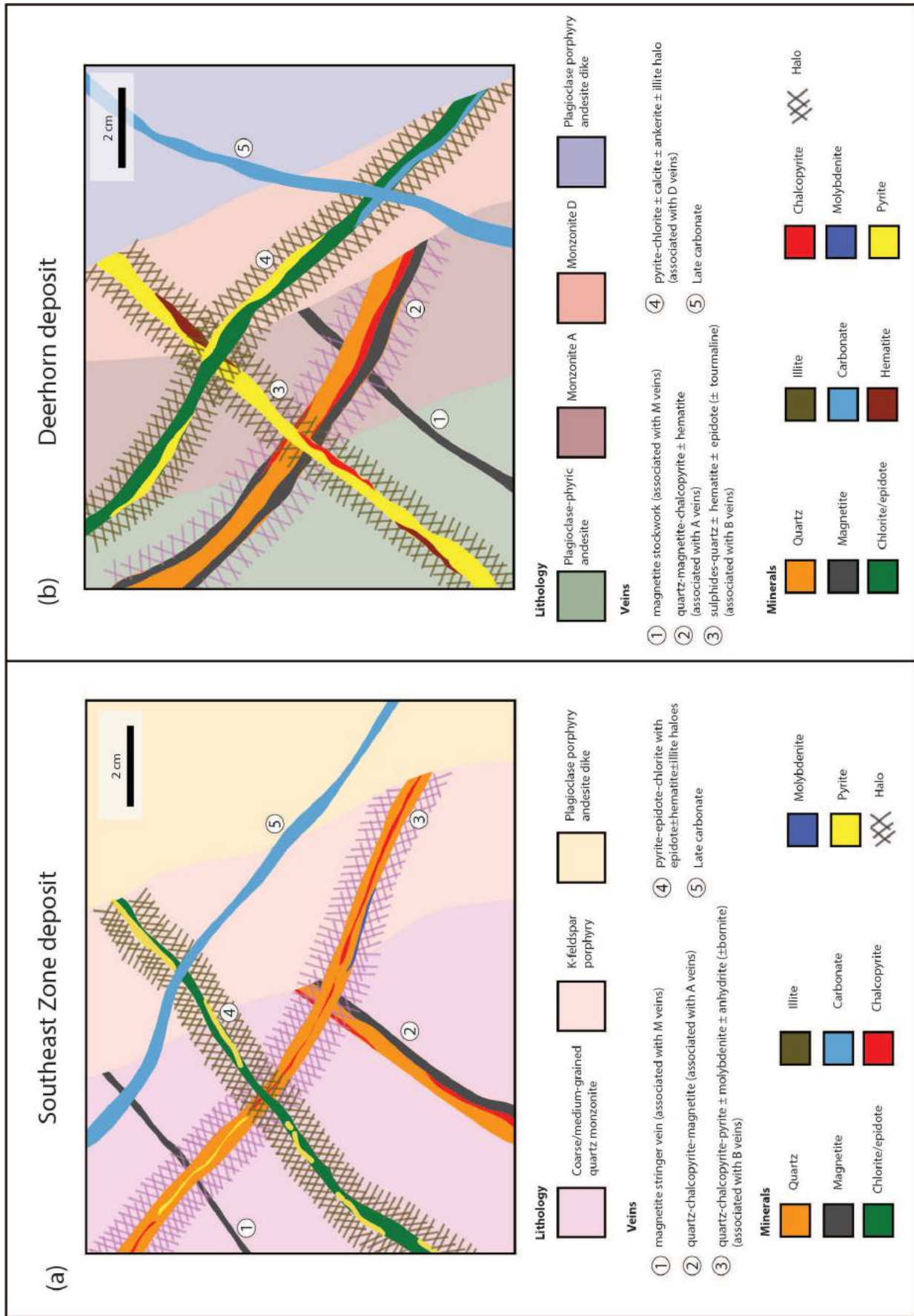


Figure 11. Summary of various vein types observed in the **a)** Southeast Zone and **b)** Deerhorn deposits, showing analogies with common vein types (e.g., M, A, B, D veins) in porphyry deposits (Gustafson and Hunt, 1975; Arancibia and Clark, 1996; Sillitoe, 2000, 2010).

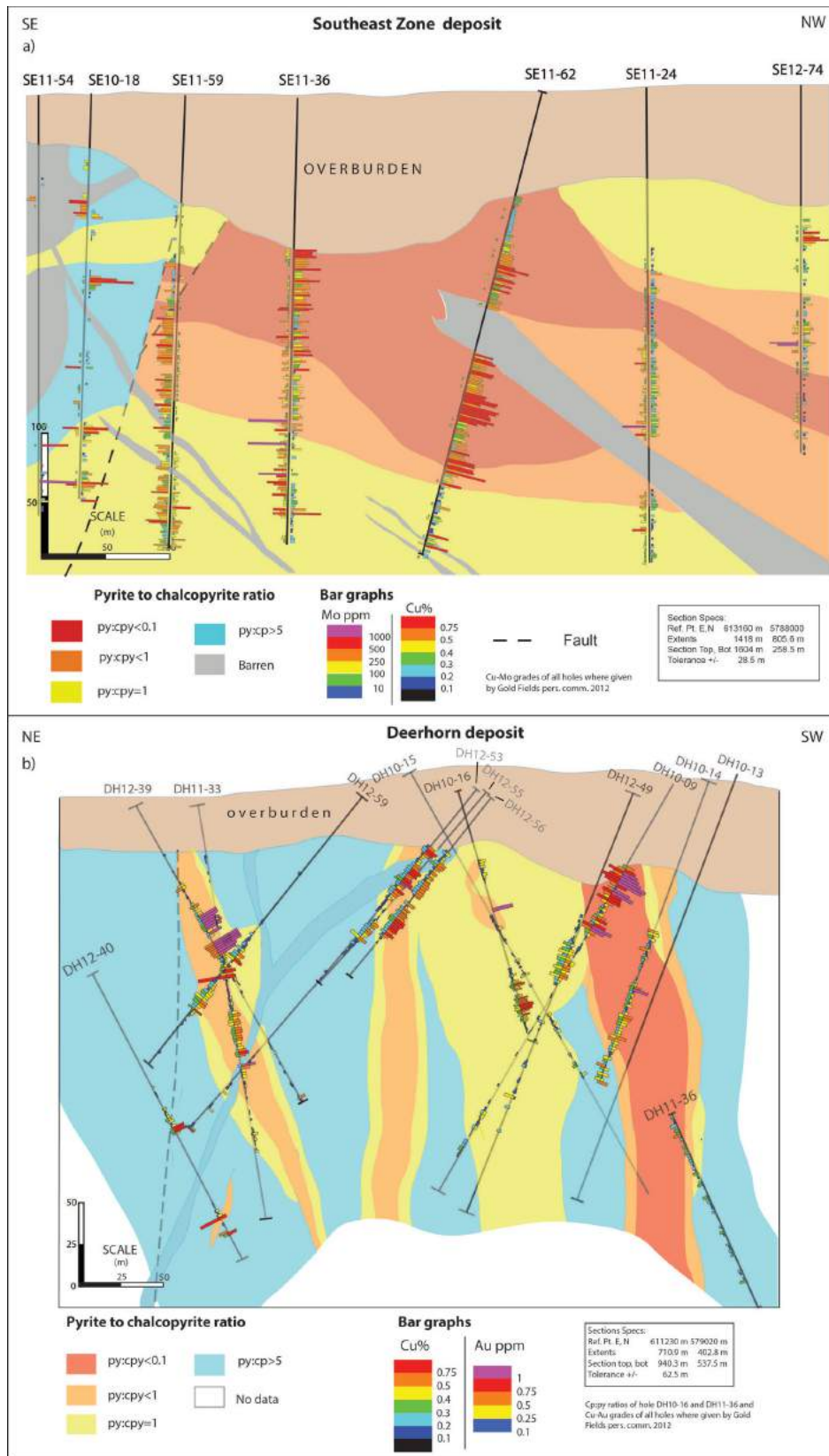


Figure 12. Sulphide ratio and Cu, Au, Mo grades for the **a)** Southeast Zone and **b)** Deerhorn deposits. Sulphide ratio calculations are based on core logging done during this study and Gold Fields Canada Exploration assay data. Copper assay values are shown on the right side of the drillhole trace for the Southeast Zone deposit and on the left side for the Deerhorn deposit; Mo on the left side of the drillhole for the Southeast Zone deposit and Au on the right side for the Deerhorn deposit.

py:cpy ratio of <0.1 ; this is attributed to the FP being a late-mineralization intrusion. The southeastern portion of the deposit has a py:cpy ratio of >5 and is locally barren in the shallower and middle portions of the drillcore from this area of the deposit (Figure 12a). This barren portion is related to intense albite alteration. In the deeper part of the deposit (350 m or more), chalcopyrite increases (py:cpy = 1) and albite alteration diminishes. This area of the deposit is interpreted as having been originally shallower in the porphyry system and later displaced by a normal fault.

Mineralization in the Deerhorn deposit differs from mineralization in the SEZ deposit in that it has significantly higher Au grades associated with Cu mineralization (up to <1.5 ppm Au and $<0.75\%$ Cu; Figure 12b). Mineralization is hosted dominantly in monzonite A (Figure 6d) and the adjacent volcanic hostrocks and occurs either as disseminations or in the early quartz-magnetite-chalcopyrite veins and later quartz veins with sulphides. Monzonite D hosts lower grades of Cu mineralization (~ 0.1 – 0.3% ; Figure 12b) but does not host significant Au. Trace amounts of molybdenite have been observed in the later-stage quartz veins with sulphides in monzonite D. Sulphide ratios are affected by hostrocks: monzonite A and immediate surrounding volcanic rocks have a py:cpy ratio of <0.1 , whereas the rest of the deposit is dominated by a py:cpy ratio of >5 (Figure 12b). Sulphide ratios, and Cu and Au grades vary in different bodies of monzonite A. For example, the monzonite A body in the southwestern part of the cross-section (Figure 12b) has a py:cpy ratio of <0.1 , whereas the other two monzonite A bodies have py:cpy ratios of <1 . A similar relationship can be seen for Au grades (Figure 12b).

Discussion

The characteristics of the hostrock, alteration and mineralization of the SEZ and Deerhorn deposits were documented on the basis of field and petrographic observations in order to understand their similarities, differences and possible genetic relationships.

The SEZ deposit is hosted in texturally variable quartz monzonite intrusive rocks that are inferred to be part of the Takomkane batholith. Alteration is zoned from intense K-feldspar–biotite–magnetite in the centre, which becomes weaker toward the margins and is laterally surrounded by albite alteration at the margins of the deposit. Epidote±chlorite±pyrite alteration overprints the K-feldspar–biotite–magnetite alteration and is locally intense at the margins of the deposit, but is weak to absent in the core. Chlorite replaces primary and secondary mafic minerals. Illite alteration occurs as an overprint of K-feldspar and plagioclase. Mineralization is zoned from chalcopyrite-bornite mineralization anomalous in Au (~ 0.2 ppm) to pyrite-dominated mineralization at the margins. However, the low abundance of quartz veining is not a typical feature of

calcalkalic deposits. Alteration and sulphide-ratio zoning suggest that the deposit has been tilted approximately 25° to the southeast, which coincides with the orientation of the basaltic dikes and the andesitic porphyry dike.

The Deerhorn deposit is hosted in a series of narrow (<100 m) monzonite intrusions that have ‘pencil’ geometries. No modal quartz is observed in the volcanic hostrocks or the monzonite intrusions. The lack of modal quartz is a common characteristic of alkalic porphyry systems in BC (Lang et al., 1995). Alteration is characterized by intense K-feldspar–biotite–magnetite in monzonite A and adjacent volcanoclastic rocks and is moderate to weak in monzonite D. Potassium feldspar–biotite–magnetite alteration is overprinted by epidote+chlorite+hematite+pyrite alteration and a later illite alteration that replaces plagioclase and overprints K-feldspar vein haloes. Calcite+ankerite+pyrite veins overprint earlier alterations. Late kaolinite alteration occurs along a main structure together with dusty hematite replacing magnetite and chalcocite replacing chalcopyrite. These observations suggest that kaolinite is a supergene alteration product(?). Mineralization is hosted in two vein stages: 1) a very dense banded and sheeted network of quartz-magnetite-hematite-chalcopyrite veins that is strongly developed in monzonite A and the adjacent volcanic hostrocks, and 2) later quartz-chalcopyrite-pyrite veins that crosscut all the hostrocks at the Deerhorn deposit, including monzonite D. The K-feldspar–biotite–magnetite alteration assemblage and the vein stages observed at the Deerhorn deposit are consistent with characteristics of Cu–Au calcalkalic porphyry systems (Sillitoe, 2000, 2010). Occurrence of tourmaline alteration (Figure 10) and minor molybdenite in monzonite D are additional features representative of a more calcalkalic system. However, the ‘pencil’-shape intrusive hostrock lacking modal quartz and laminated quartz-magnetite veins with sulphides is consistent with characteristics of Cu–Au quartz-saturated alkalic porphyry systems (Holliday et al., 2002). These observations indicate that the Deerhorn deposit has characteristics of both alkalic and calcalkalic systems; similar to those at the Red Chris deposit in northwestern BC, where the hostrock is a quartz-poor monzonite and mineralization is hosted in banded quartz veins (Norris et al., 2011). Similarly, the Skouries deposit in northern Greece occurs in a syenite that hosts Cu mineralization in banded quartz veins (Frei, 1995).

The SWIR analysis conducted in the SEZ and Deerhorn deposits distinguished different alteration mineralization styles and complemented petrographic observations. Illite was the main mineral observed in the SEZ and was classified into two major types. The first type is an illite-(muscovite) assemblage with a K-feldspar affinity that occurs at the margins of the deposit. This illite alteration is interpreted as having formed above the K-feldspar–biotite–magnetite alteration assemblage and is commonly associ-

ated with a higher concentration of pyrite. In petrographic terms, this alteration occurs as an apple-green illite replacing plagioclase and groundmass flooding. The illite-(muscovite) alteration and the K-feldspar-biotite-magnetite alteration assemblage are overprinted by a second type of illite alteration with more phengitic affinity. The phengitic illite alteration occurs as dark green illite replacing plagioclase and is interpreted as having formed at lower temperatures. Therefore, separating and mapping the various types of illite can vector toward the K-silicate alteration and higher grades. These results are comparable to the alteration observed at the Pebble porphyry deposit, Alaska (Harraden et al., 2013), in which a lower temperature illite alteration (represented as an absorption feature >2200 nm using SWIR) overprints illite-(muscovite) of the quartz-sericite-pyrite alteration assemblage with the K-rich affinity (absorption feature <2200 nm).

The results of SWIR analysis identified kaolinite and montmorillonite alteration at Deerhorn. The kaolinite alteration is structurally controlled and occurs together with dusty hematite replacing magnetite and chalcocite replacing chalcopyrite.

The next stage of this project will focus on determining the geochemistry and magmatic-hydrothermal evolution of these deposits in the Woodjam property and gaining a better understanding of the genetic relationship between the intrusive units of both deposits. Understanding the link between the two deposits will provide insight into the possible existence of a genetic relationship between alkalic and calcalkalic deposits worldwide, and will have important implications for exploration targets in the area and in other areas of BC containing intrusive bodies similar to the Takomkane batholith.

Acknowledgments

Geoscience BC is acknowledged and thanked for the funding provided for this project. Gold Fields Canada Exploration is thanked for the funding and field support for the project. The entire staff of the Woodjam project, including J. Scott, M. McKenzie, A. Ross, S. Vanderkekhove, K. Rempel and M. Eckfeldt are thanked for their support during the fieldwork. T. Bissig is acknowledged for reviewing this paper.

References

- Arancibia, O.N. and Clark, A.H. (1996): Early magnetite-amphibole-plagioclase alteration-mineralization in the Island Copper porphyry copper-gold molybdenum deposit, British Columbia; *Economic Geology*, v. 91, p. 402–438.
- Blackwell, J., Black, E. and Skinner, T. (2012): National Instrument 43-101 Technical Report on 2011 Activities on the Woodjam North Property, Cariboo Mining Division, British Columbia, 134 p.
- Casselman, M.J., McMillan, W.J. and Newman, K.M. (1995): Highland Valley porphyry copper deposits near Kamloops, British Columbia: a review and update with emphasis on the Valley deposit; *in* *Porphyry Deposits of the Northwestern Cordillera of North America*, T.G. Schroeter (ed.), Canadian Institute of Mining, Metallurgy and Petroleum, Special Volume 46, p. 161–191.
- Chamberlain, C.M., Jackson, M., Jago, C.P., Pass, H.E., Simpson, K. A., Cooke, D.R. and Tosdal, R.M. (2007): Toward an integrated model for alkalic porphyry copper deposits in British Columbia (NTS 039A, N, 104G); *in* *Geological Fieldwork 2006*, Geoscience BC, Report 2007-1, p. 259–274.
- Del Real, I., Hart, C.J.R., Bouzari, F., Blackwell, J.L., Rainbow A., Sherlock, R. and Skinner, T. (2013): Paragenesis and alteration of the Southeast Zone and Deerhorn porphyry deposits, Woodjam property, central British Columbia (parts of 093A); *in* *Geoscience BC Summary of Activities, 2012*, Geoscience BC, Report 2013-1, p. 79–90.
- Fraser, T.M., Stanley, C.R., Nikic, Z.T., Pesalj, R. and Gorc, D. (1995): The Mount Polley alkalic porphyry copper-gold deposit, south-central British Columbia, *in* *Porphyry Deposits of the Northwestern Cordillera of North America*, T.G. Schroeter (ed.), Canadian Institute of Mining, Metallurgy and Petroleum, Special Volume 46, p. 609–622.
- Frei, R. (1995): Evolution of mineralizing fluid in the porphyry copper system of the Skouries Deposit, Northeast Chalkidiki (Greece): evidence from combined Pb-Sr and stable isotope data; *Economic Geology*, v. 90, no. 4, p. 746–762.
- Gustafson, L.B. and Hunt, J.P. (1975): The porphyry copper deposit at El Salvador, Chile; *Economic Geology*, v. 70, no. 9., p. 857–312.
- Harraden, C.L., McNulty, B. A., Gregory, M.J. and Lang, J.R. (2013): Shortwave infrared spectral analysis of hydrothermal alteration associated with the pebble porphyry copper-gold-molybdenum deposit, Iliamna, Alaska; *Economic Geology*, v. 108, no. 3, p. 483–494.
- Holliday, J.R., Wilson, A.J., Blevin, P.L., Tedder, I.J., Dunham, P.D. and Pfitzner, M. (2002): Porphyry gold-copper mineralization in the Cadia district, eastern Lachlan fold belt, New South Wales and its relationship to shoshonitic magmatism; *Mineralium Deposita*, v. 37, p. 100–116.
- Lang, J.R., Lueck, B., Mortensen, J.K., Russel, J.K., Stanley, C.R. and Thompson, J.M. (1995): Triassic-Jurassic silica undersaturated and silica-saturated alkalic intrusions in the Cordillera of British Columbia: implications for arc magmatism; *Geology*, v. 23, p. 451–454.
- Logan, J.M., Mihalynuk, R.M., Friedman, R.M. and Creaser, R. A. (2011): Age constraints of mineralization at Brenda and Woodjam Cu-Mo±Au porphyry deposits—an early Jurassic calcalkaline event, south-central British Columbia; *in* *Geological Fieldwork 2010*, BC Ministry of Energy and Mines, Paper 2011-1, p. 129–144.
- McMillan, W.J., Thompson, J.F.H., Hart, C.J.R. and Johnston, S.T. (1995): Regional geological and tectonic setting of porphyry deposits in British Columbia and Yukon Territory; *in* *Porphyry Deposits of the Northwestern Cordillera of North America*, T.G. Schroeter (ed.), Canadian Institute of Mining, Metallurgy and Petroleum, Special Volume 46, p. 40–57.
- Mihalynuk, M.G., Nelson, J. and Diakow, L.J. (1994): Cache Creek terrane entrapment: oroclinal paradox within the Canadian Cordillera; *Tectonics*, v. 19, p. 575–595.

- Monger, J. and Price, R. (2002): The Canadian Cordillera: geology and tectonic evolution; Canadian Society of Exploration Geophysicists Recorder, v. 27, no. 2, p. 17–36.
- Mortimer, N. (1987): The Nicola Group: Late Triassic and Early Jurassic subduction-related volcanism in British Columbia; Canadian Journal of Earth Sciences. v. 24, p. 2521–2536.
- Norris, J.R., Hart, C.J.R., Tosdal, R.M. and Rees, C. (2011): Magmatic evolution, mineralization and alteration of the Red Chris copper gold porphyry deposit, northwestern British Columbia (NTS 104H/12W); *in* Geoscience BC Summary of Activities 2010, Geoscience BC, Report 2011-1, p. 33–44.
- Panteleyev, A., Bailey, D.G., Bloodgood, M.A. and Hancock, K.D. (1996): Geology and mineral deposits of the Quesnel River–Horsefly map area, Central Quesnel Trough, British Columbia; BC Ministry of Energy and Mines, Bulletin 97, 156 p.
- Rainbow, A. (2010): Assessment report on 2010 activities on the Woodjam South Property including soil sampling, surface rock sampling and diamond drilling; BC Ministry of Energy and Mines, Assessment Report 32 958, 1260 p.
- Rainbow, A., Blackwell, J., Sherlock, R., Bouzari, F., Skinner, T., Black, E. and Madsen, J. (2013): Geology and age relationships of contrasting styles of Cu-Mo-Au porphyry mineralization at the Woodjam Project, Horsefly, BC; Geoscience for Discovery Conference, Society of Economic Geology, Whistler, BC, September 24–27, 2013.
- Schiarizza, P., Bell, K. and Bayliss, S. (2009): Geology and mineral occurrences of the Murphy Lake area, south-central British Columbia (NTS 93A/03); *in* Geological Fieldwork 2008, BC Ministry of Energy and Mines, Paper 2009-1, p. 169–188.
- Scott, J. (2012): Geochemistry and Cu-Au mineral paragenesis of the Deerhorn prospect: Woodjam porphyry Cu-Au district, British Columbia, Canada; B.Sc. Honours thesis, University of British Columbia Okanagan, 120 p.
- Sherlock, R., Poos, S. and Trueman, A. (2012): National Instrument 43-101 technical report on 2011 activities on the Woodjam South property; Cariboo Mining Division, BC, 194 p., URL <http://sedar.com/GetFile.do?lang=EN&docClass=24&issuerNo=00032460&fileName=/csfsprod/data132/filings/01934687/00000001/y%3A%5CWeb_Documents%5CRADAR%5CE3%5CE3CO0C24%5C23JL12137%5C120723WJSTR_jaj.pdf> [November 2013].
- Sillitoe, R.H. (2000): Gold-rich porphyry deposits: descriptive and genetic models and their role in exploration and discovery; Reviews in Economic Geology, v. 13, p. 315–345.
- Sillitoe R.H. (2010): Porphyry copper systems, Economic Geology, v. 105, pp. 3-41
- Thompson, S.S.B., Hauff, P.L. and Robitaille, A.J. (1999): Alteration mapping in exploration: application of shortwave infrared (SWIR) spectroscopy; Society of Economic Geologists, Newsletter 39, p. 16–27.
- Vaca, S. (2012): Variability in the Nicola/Takla Group basalts and implications for alkali Cu/Au porphyry prospectivity in the Quesnel terrane, British Columbia, Canada; M.Sc. thesis, University of British Columbia, 163 p.

